

# Monocular 3D Pose Tracking of a Specular Object

Nassir W. Oumer

*Institute of Robotics and Mechatronics, German Aerospace Center, Münchner Str. 20, Weßling, Germany*

**Keywords:** Specular Surface, Pose Tracking, Feature Tracking, Model-based Tracking, On-orbit Satellite Servicing.

**Abstract:** A space object such as a satellite consists of highly specular surface, and when exposed to directional source of light, it is very difficult for visual tracking. However, camera-based tracking provides an inexpensive solution to the problem of on-orbit servicing of a satellite, such as orbital-life extension by repairing and refuelling, and debris removal. In this paper we present a real time pose tracking method applied to a such object under direct Sunlight, by adapting keypoint and edge-based approach, with known simple geometry. The implemented algorithm is relatively accurate and robust to specular reflection. We show the results which are based on real images from a simulation system of on-orbit servicing, consisting of two six degree of freedom robots, the Sun simulator and a full scale satellite mock-up.

## 1 INTRODUCTION

One of the challenges in computer vision is related to reflectance properties of object surfaces under direct source of lighting. A satellite is a such surface made up of mostly non-textured structural elements and partly covered with a thermal insulation such as multilayer insulation (known as MLI). Unfortunately this insulation is highly reflective and poses challenges for visual tracking. In spite of these difficulties, successful localization of a satellite provides several benefits for on-orbit servicing. In on-orbit servicing, a robot mounted on a servicer satellite, approaches a defective satellite (hereafter called client) from a certain range, and refuel, repair, maintain or even remove it from its orbit. Typical on-orbit servicing currently under development is the German on-orbit servicing mission (DEOS) shown in Fig.1. For this purpose, we estimate and track relative location of the client using monocular camera.

The methodology for visual processing of an object or a scene depends on the object or scene geometry, the environment and reflectance property. In computer vision as well as computer graphics, surfaces or objects are distinguished as a specular and lambertian surface. The reflectance property of the Lambertian surface is independent of viewing direction, while non-lambertian surfaces (Specular) are highly view point dependent. Most computer vision algorithms assume Lambertian surface and are successful in solving real world problems such as robot localization, augmented reality and visual servoing. How-



Figure 1: On-Orbit Servicing. Artistic impression of the German on-orbit servicing mission (DEOS); the robot arm mounted on a servicer satellite (right) is grasping the client satellite (left). ©SpaceTech GmbH

ever, visual algorithms developed for non-lambertian surfaces are mostly limited to laboratory and far less applied to real world problems such as visual tracking of a satellite under direct sunlight.

In this paper we present a visual tracking method that exploits edges and keypoints for localization of a satellite for on-orbit servicing. While state of the art model-based tracking methods are experimentally well verified for Lambertian surfaces under ordinary illumination, we are particularly interested to address a problem associated to specular object that goes beyond the theory of specular reflection. To that end, our contributions are mainly; (1) we combine edge and keypoint tracking methods applied to highly specular object under direct sunlight illumination, (2) we generate ground truth trajectory under realistic simulation of satellite and illumination with high power spotlight to simulate the Sun's spectrum, (3) we implement the proposed algorithm and evaluate its per-

formance (accuracy and robustness) under various motions and different levels of illumination, and (4) we compare our hybrid tracking method with edge based tracking, implemented by adapting Lie algebra tracking method (Drummond and Cipolla, 1999).

In the remaining sections of this paper, we present related current state of the art approach of combined edge and feature based tracking, and review computer vision methods for specular objects in Section 2. Section 3 presents our tracking method that integrates keypoints and edges in 2D-3D registration. Section 4 describes experimental setup used to validate the proposed method, and compares tracking results with edge based methods. Finally we summarize and conclude the paper in Section 5.

## 2 PREVIOUS WORK

In this section, we review pose estimation and structure reconstruction methods that exploit specular cues of the object, and briefly explore model-based tracking methods which utilize edge and point features of an object.

### 2.1 Pose Estimation from Specular Cues

In the context of pose estimation and surface reconstruction, there exist several contributions that deal with specular objects. The Theory of a specular geometry describes that image features exist as either real or virtual (Oren and Nayar, 1995). Real features are directly used by vision algorithms such as matching, tracking and structure from motion. Virtual features (specular cues) are specular reflections of a scene or an object features under change of viewpoint. Specular surfaces such as a glass and a smooth metal create ambiguity (actual scene point or reflection of another scene point) for visual interpretation.

Various methods have been proposed to utilize these virtual features. For example, shape and reflectance parameters can be simultaneously estimated from multiple views of an object made of single material with known lighting (Yu et al., 2004). Phong reflectance model is used to compute reflectance of the object shape modelled with triangular mesh, and minimize non-linear least square cost function over the shape and reflectance parameters. When the object is in motion, specular reflections produce 2D image motion (specular flow) (Oren and Nayar, 1995). The specular flow is mathematically related to the 3D structure of textured object or scene (Roth and Black, 2006) and provided a parametric mixture models for recovery of a surface. Most methods of shape

from specular reflection assume limited case of surfaces, in which its structure is known or qualitatively sparse, and the environment is calibrated. In contrast (Vasilyev et al., 2008) presented reconstruction approach that targets general surfaces under unknown real-world environments. They recovered 3D shape from optical flow induced by relative motion between a specular object, an observer and their environment. Similarly, (Adato et al., 2010) presented variational optical flow technique, which accounts for characteristics of specularities including parabolic singularities related to surface curvature which are hard to detect.

On the other hand, an object tracking with specular highlights (Gouiffès et al., 2006) exploits Phong's model by approximating general photometric changes with a continuous and differentiable function, approximated with first order Taylor series at a pixel point in the neighbourhood. This approach extends sparse optical flow tracking method such as (Shi and Tomasi, 1994), by compensating for illumination changes and specular highlights. In the context of pose estimation, unlike classical methods which discard lighting-information, (Lagger et al., 2008) refined coarse pose estimates by incorporating lighting information in texture and specular cues to improve accuracy of standard template matching algorithm. In this approach environment map is retrieved from the specular pixels of shiny objects and registration is performed in both image and lighting environment space.

A practical localization and pose estimation method is demonstrated by (Chang et al., 2009). They exploited environment map, specular reflections and specular flow, handling partial occlusions, background clutter and inter-reflections. Their method requires to use a calibration object such as a mirror sphere in the target scene to capture the environment map. It is, however unsuitable for human inaccessible environments such as satellite orbits.

Despite existence of several physical and geometric reflectance models of specular objects, they are rarely exploited for real world problems, mainly because of their complexity and underlying assumptions such as placement of a calibration object in the scene. For a space object such as a satellite, the appropriate reflectance model consists of specular lobe, specular spike and diffuse reflections. In the presence of geometric model of the satellite however, specular highlights, keypoints and edges of the satellite structure can be better utilized by integrating into standard model based tracking.

### 2.2 Feature-based Tracking

Edges of an image are the most suitable cues for 3D

tracking of a space object such as satellite under direct illumination and specularity. They are relatively robust to illumination change and specularity. Moreover, an accurate and a robust 3D model based tracking can be achieved by integrating keypoints and edges, also reported by (Pressigout and Marchand, 2007), (Vacchetti et al., 2004), and (Kyrki and Kragic, 2005). On one hand, interest points are well localized in textured objects and robust to some lighting changes and geometric distortions. However, they are rarely available, unstable on poorly textured objects and invariant to scale changes. On the other hand, edges are more distinctive and informative for objects with sharp edges and strong contrast changes but ambiguous in cluttered and textured objects because of strong texture and background clutter. Moreover, some edges project close to one another and create ambiguity. Therefore, the combination of edges and feature points are complementary, enabling more stable tracking with less-drift than purely edge or point feature based methods.

Very good results of combined edge and texture tracking method, which is robust to occlusion, shadow, and some specularities, are demonstrated in (Pressigout and Marchand, 2007). Our method considers the dominant specular nature of the object unlike (Pressigout and Marchand, 2007), which focuses mainly on lambertian textured surfaces containing edges. The satellite surface is mainly textureless, with some irregularities created by thermal insulation material and corners created by intersection of segments (Fig.2).

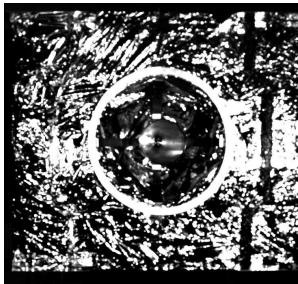


Figure 2: Specularities because of the satellite surface and direct illumination. Our region of interest for tracking is the nozzle (small circle at the center in frontal view) of the satellite. The nozzle has usually a cone or paraboloid surface geometry and is feature of most satellites.

### 3 3D TRACKING

The objective of 3D tracking of an object is to localize its position and orientation in time. In general, there exist two basic approaches of 3D tracking; model-based tracking which utilizes the CAD model of the

object, and model free tracking which does not rely on a geometric model of the object. If the model of the object is available, it provides useful prior information about the object and helps improve robustness by reducing influence of outliers on the tracker.

In this paper, we localize a space object such as satellite using model-based approach. A simple model of the object is used for absolute pose tracking, using full perspective projection camera model. The perspective projection of a 3D point  $\mathbf{p} = [X, Y, Z, 1]^T$  on image plane under pinhole camera model, is given by

$$\mathbf{x} = K[R|\mathbf{t}]\mathbf{p} \quad (1)$$

where,  $\mathbf{x}$  is an image point in homogeneous coordinate,  $K$  is a camera matrix, and  $R$  and  $\mathbf{t}$  are rotation and translation of the object in camera frame respectively. Alignment of model and image edges of non-textured object is efficiently used to recover the rotation and translation of the object, while keypoints are used for estimating this motion parameters of textured object. In this section, we present the edge based and keypoint tracking methods, and formulate the proposed hybrid feature tracking.

#### 3.1 Edge based 3D Tracking

Edges of an object are widely used feature in model-based tracking. They are mainly depth discontinuities, including object contours, segments, and primitive shapes such as circles and cylinders. For a close range (10m to 0.5m) rendezvous of a satellite, its nozzle is the most appropriate feature to track, as most satellites contain this feature to provide thrust for orbital control of the satellite. Moreover, the nozzle is frontal in this close range since the servicer and the client satellites are well aligned during mid-range (above 10m) tracking. Consequently the circular ring of the nozzle is visible in all tracking frames. Hence, our edge tracking is based on the contours of the nozzle in frontal view.

The contours (hereafter all edges are referred to as contours) are sampled and projected on to the image using hypothetical or predicted pose according to Eq. (1). Projected model points are associated to each candidate edge pixel along the respective normals, also checking against the matching edge directions (as measured by a Sobel filter), up to a reasonable threshold. The state of the art model based tracking methods (Drummond and Cipola, 2002) and (Comport and Marchand, 2004) sample contour points differently. The former samples 3D contour points and project each point to image plane while the latter samples the contours after projecting on the image plane.

The reader may refer to (Comport et al., 2005) for comparative study of the two methods.

### 3.2 Keypoint Tracking

Textured objects consist in distinctive feature points suitable for tracking. On the contrary textures are background clutters for purely edge based tracking. Despite a few in number and sparsely distributed, feature points of satellite surface are useful for tracking. Moreover, such keypoints provide additional cues to estimate correctly the 6D parameter of the motion, as 6 degree of freedom (DOF) motion can not be recovered from certain geometric primitives (e.g circle and cylinder provide only 5D parameters of 6 DOF motion of the satellite). Furthermore, when the edges are weak relative to background clutters, the edge based tracking gives rise to large errors. Hence, keypoints are vital to ameliorate robustness and accuracy of visual tracking.

As 3D keypoints of the satellite are not provided in our model, we create such model points by back-projection of detected feature points in the image, at a known pose estimated using contour based method. The alternative approach to this method is given by (Comport et al., 2005), by which they estimate homography using the pose from edge-based tracker. Our method is general, in that most satellite surfaces can be modelled with their primitive shapes such as cuboid, cylinder, cone, circle and rectangle.

For back-projection of the keypoints, we remodel the geometry of the frontal surface of the satellite (see client satellite mock-up in Fig.3), approximated with right circular cone and cuboid. Although there exist small unknown curvature at the center of the cuboid, the model is good approximation to the structure of the satellite. Accordingly, we compute the 3D points corresponding to image keypoints through ray intersection. A ray passing through the image point  $\mathbf{x} = [u, v]^T$  intersects either a cuboid of known size with normal  $\mathbf{N}$  or the right circular cone, parametrized by

$$\begin{aligned} (X - V)^T M (X - V) &= 0 \\ A \cdot (X - V) &\geq 0 \\ M &= AA^T - \cos(\theta)^2 I \end{aligned} \quad (2)$$

, where  $A$  is a direction of the cone axis,  $\theta$  is an acute angle of the cone, which is the angle between axis of the cone and a ray through the point  $X$  on the surface of the cone and the vertex  $V$ , and  $I$  is identity matrix.

After we create 3D model points, the detected keypoints are tracked using KLT tracker (Shi and Tomasi, 1994). Unreliable features are automatically rejected and substituted by new features during tracking. When the 3D model points are not sufficient as

a result of feature rejection, we create model points from the newly detected features.

### 3.3 Hybrid Feature Tracking

As stated earlier in this paper, integrating edge and point features (Fig.4) into 3D tracking corrects drawbacks of a solely edge-based or feature point tracking. In this section, we present the registration of edge and feature point cues within the same minimization process, by utilizing 3D point models created by ray tracing and 3D contour points of a satellite. The 3D tracking approach is differently handled for the features obtained from keypoints and edges; matching points of the projected contour points are searched along the edge normals (1D search) while matching feature points is 2D search. Thus we treat joint optimization of the cost function associated to these features in different direction.

Let  $\delta\mathbf{p}$  be inter-frame motion. The rigid body tracking is tantamount to computing the transformation matrix  $T$  in time  $t$  for the motion model, provided the last transformation at time  $t - 1$ , according to

$$T_t = T_{t-1} \delta T(\delta\mathbf{p}_t) \quad (3)$$

where the incremental transform  $\delta T$  is singularity-free around  $\delta T(\delta\mathbf{p} = 0)$ . The tangent space to  $SE(3)$  at  $T_{t-1}$  is given by the Lie algebra  $se(3)$ , which provides  $\delta T$  through the exponential mapping

$$\delta T(\delta\mathbf{p}) = \exp\left(\sum_{i=1}^6 G_i \delta p_i\right) \quad (4)$$

where  $G_i$  are the canonical  $(4 \times 4)$  generators of  $se(3)$  (Drummond and Cipolla, 1999).

Each 3D point  $X$ , obtained by ray tracing and sampling on the contour, is projected onto image point  $\mathbf{y}$  by the respective  $(3 \times 4)$  camera matrix  $K$

$$\mathbf{y} = \pi(K \cdot T \cdot \delta T(\delta\mathbf{p}) \cdot X) \quad (5)$$

where the operator  $\pi(\cdot)$  transforms from homogeneous to Euclidean 2D coordinates

$$\pi(z) = \begin{bmatrix} \frac{z_1}{z_3} & \frac{z_2}{z_3} \end{bmatrix}^T. \quad (6)$$

We minimize the joint objective function

$$\arg \min_{\delta T} \sum_i \rho \left( \left( \mathbf{x}_i^{edge} - \mathbf{y}_i(\delta T) \right)^2 + \left( \mathbf{x}_i^{point} - \mathbf{y}_i(\delta T) \right)^2 \right) \quad (7)$$

where  $\rho(\cdot)$  is a robust function,  $\mathbf{x}_i^{edge}$  and  $\mathbf{x}_i^{point}$  are edge and tracked feature points respectively.

Differentiating Eq.(5) with respect to incremental pose parameters  $\delta p_i$  as

$$\frac{\partial \mathbf{y}}{\partial (\delta p_i)} \Big|_{\delta \mathbf{p}=0} = \frac{\partial \pi}{\partial \mathbf{z}} \Big|_{\mathbf{z}=KTX} \cdot K \cdot J^i, \quad (8)$$

gives rise to screen Jacobian, where  $J^i$  is the transformation Jacobian, given by the respective generator

$$J^i = T \frac{\partial}{\partial(\delta p_i)} \delta T(\delta \mathbf{p}) \Big|_{\delta \mathbf{p}=0} = T G_i. \quad (9)$$

The screen Jacobian of each contour point in the direction of screen normal  $\mathbf{n}$  is stacked, to form the Jacobian  $J_{edge}$ , of maximum size  $(n_p \times 6)$ . Similarly, the Jacobian  $J_{point}$  associated to re-projection error of 3D point models (from ray tracing) is computed, in this case without screen normal as these model points are not contour points. Hence, overall Jacobian ( of size  $3n_p \times 6$ ) of the minimization is derived by cascading

$$J = [ J_{edge} \quad J_{point} ]^T. \quad (10)$$

Thus, pose parameters  $\delta \mathbf{p}$  are updated by minimizing residuals  $\mathbf{r}$ , given by

$$\mathbf{r} = [ \mathbf{y}_i^T \mathbf{n}_i \quad u_i - x_{2i} \quad v_i - y_{2i} ] \quad (11)$$

where  $\mathbf{x} = [u_i, v_i]^T$  are tracked image feature points,  $x_{2i}$  and  $y_{2i}$  are projections of 3D points onto the image plane expressed in standard coordinate.

Several background clutters exist because of specular reflections, resulting very similar edges to the nozzle edge. Hence, the tracker should be robust to outliers. The robust function  $\rho()$  in Eq.(7) provides such functionality to reject spurious features during tracking. For real time efficiency we choose the M-estimator adopted in the context of 2D visual servoing (Comport et al., 2006). The M-estimator adaptively thresholds outliers based on robust statistics, while re-weighting inliers according to the Tukey bi-weight function

$$w_i = \left( b^2 - \left( \frac{r_i - \bar{r}}{\sigma} \right)^2 \right)^2 \quad \text{if} \quad |r_i - \bar{r}| < b\delta \quad (12)$$

and otherwise the weight is set to zero, where  $b = 4.6851$  is the threshold for Tukey's function, and the scale  $\delta$  is the standard deviation of inlier data, robustly estimated using the median of absolute deviations (MAD) from the median residual  $\bar{r}$ , and used to compute the weights. Re-weighted least square minimization is performed, by Gauss-Newton update according to the Eq.(13)

$$\delta \mathbf{p} = (J^T W J)^{-1} J^T W \mathbf{r} \quad (13)$$

where  $W$  is a diagonal matrix containing all weights, and iterated with the new  $T$  matrix, computed by Eq. (3), until the increment is sufficiently small.

This general formulation can be applied also to cases with reduced degrees of freedom, by suppressing the Jacobian column related to some of the generators  $G_i$ . Moreover, for our scenario rotation is controlled quite precisely through attitude measurements



Figure 3: DLR on-orbit servicing simulation system consists of two robots and a satellite mock-up (client). The servicer (left) and the client with its nozzle(right).

used for control of the satellite, thus we only show results concerning pure translation and oscillations, by fixing the rotational part  $R$  and using the other three generators.

## 4 EXPERIMENTAL RESULTS

In this section, we present the experimental setup and some of our results at various illumination level and motion trajectories. As our objective is to address real world problem of visual tracking, the experiment is performed with one of the most realistic space simulation system. This system (Fig.3) consists of a high power floodlight (the Sun simulator), client satellite covered with thermal protection (such as multilayer insulation, MLI) which is highly reflective, two 6 DOF Kuka robot system to reproduce relative motion of servicer and client satellites. The reflective surface of the client, illuminated with direct Sun light produces strong specular reflections (see Fig.2), located on irregular corners and edges. Although these image features are short-lived and have unstable shape and size, we are able to achieve reasonable accuracy and robustness.

We performed the experimentation with various motions to validate the method and demonstrate the practicality. The ground truth data is generated through robot measurements and hand-eye camera calibration (DLR Callab toolbox). The maximum translational and angular velocities are 5cm/s and 1deg/s respectively. The motion is mainly oscillatory with small rotation. The two satellites are assumed controllable, hence relative attitude measurements can be provided with external system. Consequently we focus on oscillatory motion of the client in this experiment. However, the implemented algorithm can provide poses for 6 DOF motion. We initialized the tracker manually, which can be also provided by an external tracker used for mid-range ( $\geq 10$ m) localization. The implementation is in C++, while opencv is used for low-level processing such

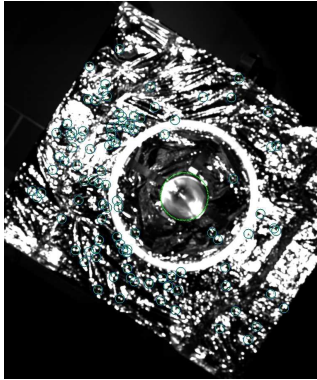


Figure 4: Combined edge and feature point tracking for 3D localization. Keypoints (small green circles) of irregular surface and circle of the nozzle (green contour) are tracked.

as edge detection and point feature tracking. The average processing time for image size of 1024x1024 is 135ms on 2.8GHz processeor.

Hereafter we present experimental results of four trajectories among our several trajectories (with various motion, illumination level and the Sun direction), and compare combined edge and feature point tracking with edge based tracking. Fig.5 illustrates one of the ground truth and the estimated trajectories. In the first test trajectory, the client moves from 5m to 1m in Z-direction and from 1m to 0 in X-direction linearly. It rotates around X-axis with sinusoidal oscillation and around Z-axis with linear rotation. The ground truth error associated to hybrid and edge based tracking is shown in Fig.6; the dominant motion (of all trajectories) is along camera Z-axis, hence we discuss errors in this direction and compare translation errors by combined edge and feature point tracking, and edge based tracking method. The error of combined edge and keypoint tracking is relatively smaller, when the client is close to the camera and far away (at the beginning). However, the edge based tracking outperforms combined edge and feature point tracking around the middle of the trajectory (3m to 2m range). We explain why such error variation occurred, shortly after we demonstrate results of other trajectories.

Also we observe similar error distribution in Fig.7, of which the translation motion of the client is similar to above except the rotation, which is only around X-axis alternating with sinusoidal motion. In contrast, when the client motion is purely translational without oscillation, the error of hybrid tracking is relatively smaller at the beginning and larger around the middle of the trajectory, similar to the rest of the experiment. At very closer range however the error of the hybrid tracking is approximately comparable to edge based tracking ( Fig.9) unlike that of other experiments. We would like to remark that all the above

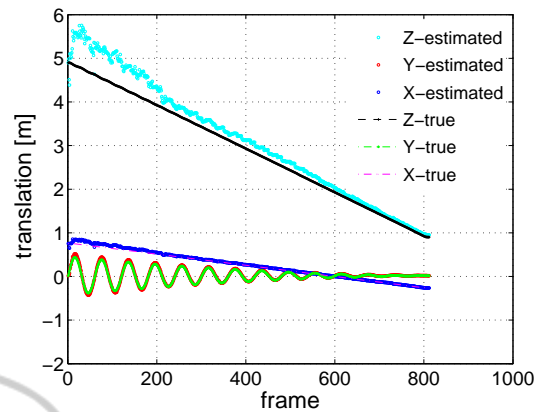


Figure 5: One of the ground truth trajectories used for validation and corresponding estimated trajectory of the client.

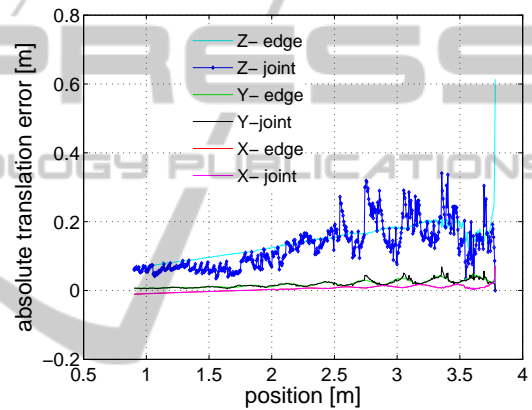


Figure 6: Comparison of ground truth errors of hybrid (joint keypoint and edge) and edge based tracking. The motion is linear translation along Z- and X-axis while oscillating sinusoidally in X-axis and small linear rotation about Z-axis.

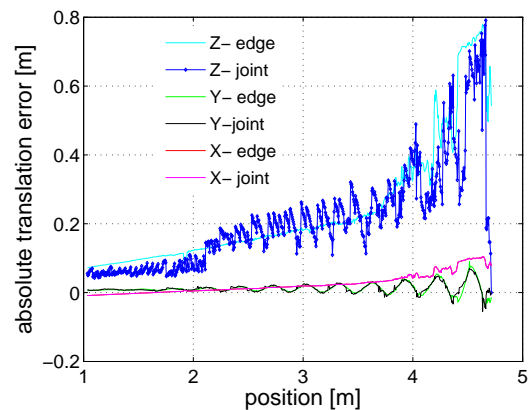


Figure 7: Ground truth errors of hybrid and edge based tracking. The motion is similar to that of Fig.6 except the client rotates only around X-axis alternating sinusoidally.

experiments are performed while the direction of the Sun simulator is perpendicular to the camera axis. On the other hand, the ground truth error of a motion tra-

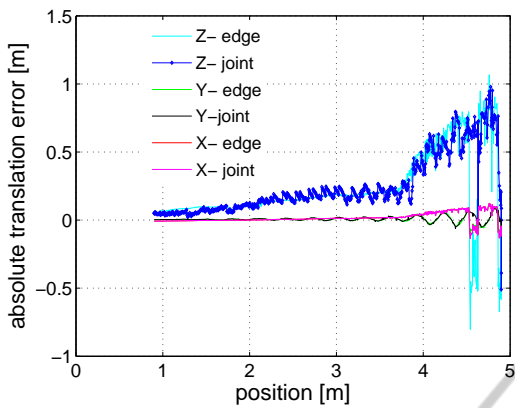


Figure 8: Comparison of ground truth errors of trajectory similar to that of Fig.7 but with higher illumination and different direction (60 deg) of the Sun simulator.

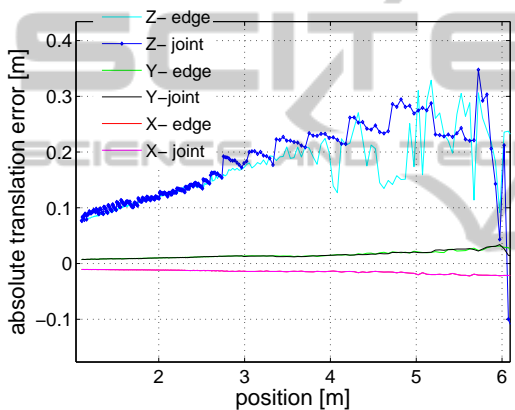


Figure 9: Ground truth errors of purely translational motion. Edge based tracker provides approximately the same errors as that of hybrid tracking while the former outperforms the latter around the middle of trajectory for a such simple motion.

jectory similar to Fig.7, but the direction of the Sun simulator about 60 deg to camera axis and illumination level 10 % higher, is shown in Fig.8. In spite of the change of the illumination and direction of source of light, the error of hybrid tracking is comparatively smaller than that of edge based tracking around similar regions within the close-range described above.

Combined edge and keypoint tracking outperforms edge based tracking in ambiguous region of the tracking, where the contrast of the nozzle is very low. The edges extracted from the nozzle of the satellite around 4m are very similar to background edges, and difficult to track with edge based tracker. In contrast, there exist distinctive point features because of irregular surface of the MLI, which provide important cues for tracking. Thus, the tracking benefits from combined keypoint and edges. On the other hand, at closer range (around 2m) the edge of the nozzle of the satellite, is sharp with good contrast and can be eas-

Table 1: RMS errors of the edge based and hybrid feature tracking for various trajectories. The error is in m. The hybrid feature tracking outperforms the edge based tracking.

Trajectory	Edge	Hybrid
1	0.1485	<b>0.1432</b>
2	0.2978	<b>0.2606</b>
3	0.1445	0.1470
4	0.3471	<b>0.3297</b>

ily tracked, however, is not fully visible in the camera field of view. The sharp contours of the nozzle and distinctive feature points at very close range provide strong cues for accurate and robust tracking. On the contrary, the accuracy of the combined edges and point tracking in the range around 4m to 2m drops compared to edge based tracking. This is simply because, feature points are not well localized and drift quickly. The drift also causes the optimization to converge to local minima, degrading the performance of the overall hybrid tracking. Thanks to model based absolute pose tracking, the drift does not accumulate and recovers to the correct pose when good features and edges are detected in the subsequent frames. In general, the accuracy of the hybrid tracking is better than the solely edge-based tracking, as demonstrated with root mean square errors of each test trajectory in Table 1.

## 5 CONCLUSIONS

We implemented a hybrid tracking method that exploits image edges and feature points, and demonstrated experimental results under challenging illumination condition (directional Sunlight) and visually difficult reflective surface (satellite). Simple geometric features such as depth discontinuities and primitive shapes on the satellite provide strong cues for real time tracking, and are efficient to compute on standard processor. Although such features of Lambertian object are salient under normal lighting, they are often ambiguous against background clutters for specular objects under direct illumination. The ambiguity is resolved by combining contours and point features to ameliorate robustness and accuracy. Our extensive experimentation using camera images, the Sun simulator, satellite mock-up and simulated motion (with robots) shows relatively robust and accurate result compared to a standard edge based tracking. The tracking result can be used for approach of a client satellite for on-orbit servicing such as refuelling and repairing.

Despite the reported improvements, in a few cases drift of point features can prohibit the utmost ben-

efit of the hybrid tracking. However, drift free (at least, reduced drift) feature-based tracking, can be integrated into edge based tracking. Moreover, our experiment is based on translational motion with small rotation and oscillation. Large rotation causes large change of view and the feature points even drift more. In the future work we will address this large drift of point features, rotational motion due to tumbling satellite and illumination changes.

## ACKNOWLEDGEMENTS

The author would like to acknowledge Dr. Giorgio Panin and Dr. Toralf Boge for their invaluable support.

## REFERENCES

- Oren Michael and Nayar Shree K. (1995). A Theory of Specular Surface Geometry. In *IJCV'95, International Journal of Computer vision*, volume 24, page. 740–747.
- Lagger Pascal, Salzmann Mathieu, Lepetit Vincent and Fua pascal (2008). 3D Pose Refinement from Reflections. In *CVPR'08, IEEE Conference on Computer vision ans Pattern Recognition*, pages 1-8, Anchorage, AK.
- Yu Tianli, Xu Ning and Ahuja Narendra, (2004). Recovering Shape and Reflectance Model of Non-lambertian Objects from Multiple Views. In *CVPR'04, Proceedings of IEEE Computer Sosciety Conference on Computer vision ans Pattern Recognition*, volume 2, pages II-226 - II-233.
- Roth Stefan and Black Michael J., (2006). Specular Flow and the Recovery of Surface Structure. In *CVPR'06, Proceedings of IEEE Computer Sosciety Conference on Computer vision and Pattern Recognition*, volume 2.
- Vasilyev Yuriy, Adato Yair, Zickler Todd and Ben-Shahar Ohad, (2008). Dense Specular Shape from Multiple Specular Flows. In *CVPR'08, Proceedings of IEEE Computer Sosciety Conference on Computer vision ans Pattern Recognition*.
- Adato Yair, zickeler Todd and Benn-Shahr Ohad, (2010) Toward robust Estimation of Specular Flow. In *BMVC'10, Proceedings of the British Machine Vision Conference*, pages 22.1–22.11.
- Gouiffès Michèle, Collewet Christophe, Fernandez-Maloigne Christine, Trémeau Alain, (2006) Feature Points Tracking: Robustness to Specular Highlights and Lighting Changes. In *ECCV'06, 9th European Conference on Computer Vision*, volume 4. pages 82-93.
- Shi Jianbo and Tomasi Carlo, (1994) Good Features to Track. In *CVPR'94, IEEE Computer Soc. Conference Computer Vision and Pattern Recognition*, pages 593-600.
- Chang Ju Yong, Raskar Ramesh and Agrawal Amit K., (2009) 3D Pose Estimation and Segmentation using Specular Cues. In *CVPR'09, IEEE Computer Soc. Conference Computer Vision and Pattern Recognition*, pages 1706-1713.
- Vacchetti Luca, Lepetit Vincent, Fua Pascal, (2004) Combining Edge and Texture Information for Real-Time Accurate 3D Camera Tracking. In *ISMAR '04, Proceedings of the 3rd IEEE/ACM International Symposium on Mixed and Augmented Reality Pages 48-57*.
- Kyrki Ville, Kragic Danica (2005) Integration of model-based and model-free cues for visual object tracking. In *ICRA05, Proc. of the IEEE Int. Conf on Robotics and Automation*, pages 1554–1560.
- Pressigout Muriel and Marchand Eric, (2007) Real-time Hybrid Tracking using Edge and Texture Information. In *Proc. of International Journal of Robotics Research*, volume 26, no.7, pages 689-713.
- Drummond Tom and Cipolla Robert, (2002) Real-time visual tracking of complex structures. In *PAMI'02 Proc. of IEEE Transactions on Pattern Analysis and Machine Intelligence*, Volume 27, issue 7, pages 932 - 946 .
- Comport A.I. and Marchand Eric, (2004) Robust model-based tracking for robot vision. In *IROS'04 Proc. IEEE/RSJ International Conference on Intelligent Robots and Systems*, volume 1, pages 692 - 697.
- Comport Andrew.I., Kragic Danica, Marchand Eric and Chaumette Francois, (2005) Robust Real-Time Visual Tracking: Comparison, Theoretical Analysis and Performance Evaluation. In *ICRA'05 Proc. IEEE International Conference on Robotics and Automation*, pages 2841 - 2846.
- Comport Andrew I., Marchand Eric and Chaumette Francois, (2006) Statistically Robust 2D Visual Servoing. In *IEEE Transactions on Robotics* volume 22, no.2, pages 415-421.
- Drummond Tom and Cipolla Robert, (1999) Visual Tracking and Control using Lie Algebras. In *CVPR'99, IEEE Computer Society, Computer Vision and Pattern Recognition*, volume 2, pages 2652-2659.